Western University

Scholarship@Western

Electrical and Computer Engineering Publications

Electrical and Computer Engineering Department

Summer 7-28-2005

Study of System Parameters and Control Design for a Flexible Manipulator using Piezoelectric Transducers

Mehrdad Kermani Ph.D., P.Eng.
Western University, mkermani@eng.uwo.ca

Mehrdad Moallem
Simon Fraser University, mehrdad_moallem@sfu.ca

Rajni Patel
Western University

Follow this and additional works at: https://ir.lib.uwo.ca/electricalpub

 Part of the Computer Engineering Commons, and the Electrical and Computer Engineering Commons

Citation of this paper:
Kermani, Mehrdad Ph.D., P.Eng.; Moallem, Mehrdad; and Patel, Rajni, "Study of System Parameters and Control Design for a Flexible Manipulator using Piezoelectric Transducers" (2005). *Electrical and Computer Engineering Publications*. 551.
https://ir.lib.uwo.ca/electricalpub/551

Study of System Parameters and Control Design for a Flexible Manipulator using Piezoelectric Transducers

M.R. Kermani†, M. Moallem‡, R.V. Patel§

Department of Electrical and Computer Engineering,
University of Western Ontario,
London, ON, Canada, N6A 5B9.

E-mail: †mkermani@uwo.ca, ‡mmoallem@engga.uwo.ca, §rajni@eng.uwo.ca

Abstract. In this paper, a nonlinear control scheme is presented to achieve small tracking errors in a 2-DOF flexible manipulator. A secondary actuation mechanism using piezoelectric materials is added to the system for suppressing residual vibrations at the end point of the flexible link. A small piece of piezoceramic is also used, as a sensor, in order to obtain the modal states of the system. The effects of changing physical parameters such as relative thickness of the piezoelectric ceramic with respect to the flexible link, the optimum location and the length of the actuator are studied based on the singular value decomposition of the controllability Grammian of the system. It is shown that for each of the aforementioned parameters, an optimum value can be found which maximizes the singular value associated with one vibration mode. A partial feedback linearization technique based on output redefinition is utilized to obtain an appropriate control output for each joint and the piezoelectric actuator. A model for friction is obtained and included in the control law. Experimental results show that applying the suggested control scheme results in smooth and precise motion of the flexible manipulator without exciting unwanted vibration modes. Comparisons are made when a linear control scheme is used for the tracking problem.

1. Introduction

There has been a tremendous growth in the development of new actuator technologies in the past few years. The new actuators have been used in diverse applications. Amongst them, vibration suppression of flexible structures has received considerable attention in such applications as robotics, biotechnology and aviation [4]. To this end, many researchers have concentrated on dynamic modeling of piezoelectric (PZT) materials as elements of intelligent structures [2] [12], while a number of others have focused on control methods of piezoelectric actuators for suppressing vibrations and reducing noise [1]. Sun and Mills [14] conducted studies on the application of segmented PZT ceramics and Poly Vinylidene Fluoride (PVDF) materials for this purpose. Patnaik [10] studied stability issues in controlling a flexible beam. Hanagud

§ This research was supported in part by grants RGPIN227612 and RGPIN1345 from the Natural Sciences and Engineering Research Council (NSERC) of Canada and the Canada Foundation for Innovation (CFI) under the New Opportunities Program.

[4] investigated the possibility of using piezo-stack actuators for controlling vibrations in a fuselage. A comprehensive literature review is given in [12].

Achieving precise, fast and smooth manipulation with lightweight structures (e.g., flexible-link manipulators) is a challenging objective in today's control applications. These structures, due to their flexibility, are under-actuated. As a result, controlling such systems with the above requirements and a limited amount of control effort is in general difficult. Adding secondary actuation mechanisms such as piezoelectric materials helps to overcome these difficulties. In selecting a PZT actuator for vibration control, it is useful to know how the physical parameters of the PZT and its location can affect system performance in order to make use of its maximum strength. In this regard, the authors have attempted to address the selection process for PZT actuators using the controllability Grammian concept [6]. This paper promotes the above idea in a practical setting where piezoelectric materials are used for suppressing vibrations in a 2-DOF flexible-link manipulator for precise motion control.

The organization of this paper is as follows. In section 2, the dynamic model of a 2-DOF flexible manipulator actuated with piezoelectric transducers is reviewed. A generalized control scheme for a class of nonlinear flexible-link systems is discussed in section 3, following a discussion on actuator sizing and placement to achieve optimum controllability. In section 3 a friction compensation scheme is also presented. Finally, in section 4 experimental results are presented and further compared with the case when a linear controller is used.

2. System Modeling

Consider a 2-DOF flexible-link manipulator (Figure 4) consisting of a flexible beam clamped to the hub of a rotary motor where the whole mechanism of the beam and rotary motor is mounted on top of a linear motor moving along a track. Different methods can be used to obtain a finite-dimensional model of such a flexible-link manipulator. The most commonly used method to obtain a discrete model is based on the Raleigh-Ritz expansion [11]. It is assumed that the transverse motion of the beam can be expressed in terms of the mode shapes as follows:

$$\delta(x,t) = \sum_{i=1}^{\infty} \varphi_i(x) q_i(t) \tag{1}$$

where $\delta(x,t)$ is the transverse displacement, q_i is generalized displacement and φ_i is the mode shape of free vibrations, which can be any function that satisfies the geometrical boundary conditions. The Lagrangian formulation is probably one of the most popular methods used to develop a discrete model for a flexible structure. It is based on the energy of the system and is relatively easy to apply. Assuming a generalized displacement vector composed of the linear displacement of the linear motor $\theta_1[\mathsf{m}]$, the angular displacement of the rotary motor $\theta_2[\mathsf{rad}]$, and the first n components of $q(t)$, i.e.,

$$r = (\theta_1, \theta_2, q_1, \ldots, q_n)^T \tag{2}$$

and applying the Lagrangian formulation given by:

$$\frac{d}{dt}\left(\frac{\partial \mathcal{L}}{\partial \dot{r}}\right) - \frac{\partial \mathcal{L}}{\partial r} = \tau \tag{3}$$

the dynamic equations of the system can be obtained. In the above equation, $\mathcal{L}$ is the difference between the total kinetic energy and the potential energy of the system. Considering a pair of PZT actuators with their two ends located at distances x_a and x_b from the root position of the beam, the dynamic equations of the system are given by:

$$M(r)\ddot{r} + V(r,\dot{r}) + Kr = \tau \tag{4}$$

where

$$M(r) = \begin{pmatrix} \Phi_{\theta\theta} & \Phi_{\theta q} \\ \Phi_{\theta q}^T & \Phi_{qq} \end{pmatrix} \quad K = \begin{pmatrix} 0 & 0 \\ 0 & \Omega \end{pmatrix} \tag{5}$$

$$\Phi_{\theta\theta}(1,1) = M_h + \rho AL$$

$$\Phi_{\theta\theta}(1,2) = \Phi_{\theta\theta}(2,1) = -\rho A(\frac{L^2}{2}\sin\theta_2 + q^T\Phi_\Delta\cos\theta_2)$$

$$\Phi_{\theta\theta}(2,2) = J_h + \rho A(\frac{L^3}{3} + q^T\Phi_{qq}q) + \rho_z A_z\frac{x_b^3 - x_a^3}{3}$$

$$\Phi_{\theta q}(1,i) = -\rho A\Phi_\Delta(i)\sin\theta_2$$

$$\Phi_{\theta q}(2,i) = \rho A\int_0^L x\varphi_i(x)dx + 2\rho_z A_z\int_{x_a}^{x_b} x\varphi_i(x)dx$$

$$\Phi_{qq}(i,j) = \rho A\int_0^L \varphi_i(x)\varphi_j(x)dx + 2\rho_z A_z\int_{x_a}^{x_b}\varphi_i(x)\varphi_j(x)dx$$

$$\Phi_\Delta(i) = \rho A\int_0^L \varphi_i(x)dx + 2\rho_z A_z\int_{x_a}^{x_b}\varphi_i(x)dx$$

$$\Omega(i,j) = EI\int_0^L \varphi_i''(x)\varphi_j''(x)dx + E_z I_z\int_{x_a}^{x_b}\varphi_i''(x)\varphi_j''(x)dx$$

$V(r,\dot{r})$ is the vector of Coriolis and centrifugal forces:

$$V(r,\dot{r}) = \begin{pmatrix} v_\theta \\ v_q \end{pmatrix} = \\ -\rho A\dot{\theta}_2\begin{pmatrix} (\dot{\theta}_2\frac{L^2}{2} + 2\dot{q}^T\Phi_\Delta)\cos\theta_2 - \dot{\theta}_2 q^T\Phi_\Delta\sin\theta_2 \\ -2\dot{q}^T\Phi_{qq}q \\ \dot{\theta}_2\Phi_{qq}q \end{pmatrix} \tag{6}$$

and τ is the vector of the input torques, provided by each motor and the PZT actuators:

$$\tau = \begin{pmatrix} \tau_{motor} \\ \tau_z \end{pmatrix} \tag{7}$$

In the above formulas, ρA is the mass per unit length of the beam, $\rho_z A_z$ is the mass per unit length of the PZT, M_h is the mass of the motor hub, E and E_z are the moduli of elasticity of the beam and the PZT ceramic respectively, $I = w\frac{t_h^3}{12}$ and

$I_z = 2(\frac{t_h^2 t_z}{4} + \frac{t_h t_z^2}{2} + \frac{t_z^3}{3})$ are the moments of inertia of the cross section of the beam and the PZT respectively, J_h is the motor inertia, L, w and $t_h = 2h$ are the length, the width and the thickness of the beam, respectively and t_z is the thickness of the PZT.

The induced torque of the PZT is a function of the voltage $v(t)$ applied to the actuator. The modal elements of this torque can be obtained by initially deriving the relationship between the voltage $v(t)$ and the moment generated by the PZT. This approach follows the procedure presented in [13]. It can be shown that the moment ϵ_τ induced by a single PZT actuator per unit length of the beam is as follows:

$$\epsilon_\tau(x,t) = K_z[H(x-x_a) - H(x-x_b)]v(t) \tag{8}$$

$$K_z = -E\frac{P}{1-P}\frac{2}{3}wh^2\frac{d_{31}}{t_z}$$

$$P = \frac{-3ht_z(t_z+2h)}{2(h^3 + \frac{E_z}{E}t_z^3) + 3\frac{E_z}{E}ht_z^2}\frac{E_z}{E}$$

where d_{31} is the electrical displacement constant of the PZT, x_a and x_b are the distances from the two ends of the PZT actuator to the clamped end of the beam and $H(x)$ is the unit step function. The second partial derivative of the induced moment with respect to x, i.e. $\frac{\partial^2 \epsilon_\tau(x,t)}{\partial x^2}$, appears in the dynamic equation of a cantilevered beam, and the modal elements of the PZT torque with respect to each vibration mode can be obtained as follows:

$$\tau_z = \Delta v(t) = (\Delta_1, \ldots, \Delta_n)^T v(t) \tag{9}$$

where

$$\Delta_i = K_z\Big(\varphi_i'(x_a) - \varphi_i'(x_b)\Big) \qquad i = 1, ..., n$$

In order to obtain the modal states of the system a small piece of piezo-ceramic is bonded to the beam as a sensor. This sensor produces a charge proportional to the strain. The output charge of each sensor is fed to a charge amplifier. Hence, the output voltage of the charge amplifier measures the strain produced along the sensor in the beam. The relationship between the charge distribution and strain in a piezoelectric material is given by:

$$D = d_{31}\sigma = d_{31}E_z S \tag{10}$$

where D is the charge distribution per unit area of the sensor, σ is the stress and S is the longitudinal strain. The ceramic used as a sensor has the same material as PZT actuators; therefore E_z and d_{31} are as defined above. Since the sensor is bonded to the beam, the amount of strain developed along the sensor is equal to the strain of the beam. It is also known that the strain at each cross section of the link can be obtained by multiplying the rotation angle of the cross section by half the thickness of the link (i.e. $\frac{t_h}{2}$). Therefore the total strain produced along the sensor can be written as:

$$S = \frac{t_h}{2}\int_{x_1}^{x_2}\frac{\partial^2}{\partial x^2}\delta(x,t)dx = \frac{t_h}{2}\int_{x_1}^{x_2}\frac{\partial^2}{\partial x^2}\big(\Sigma_{j=1}^n \varphi_j(x)q_j(t)\big)dx \tag{11}$$

where x_1 and x_2 are the two ends of the piezo-sensor along the beam. The total output voltage of the charge amplifier can be obtained after dividing the total produced charge by the sensor capacity as follows:

$$v_s = \frac{d_{31} E_z t_h w_s}{2C_s} \int_{x_1}^{x_2} \Sigma_{j=1}^{n} \big(\frac{\partial^2 \varphi_j(x)}{\partial x^2} q_j(t) \big) dx \tag{12}$$

where w_s is the width and C_s is the capacitance of the sensor. All other parameters are as defined previously. As observed, equation (12) provides a weighted sum of all vibration modes of the system. However, in the frequency domain and for free vibration of the link, the information about each mode can be extracted from the original signal using appropriate filtering methods. Furthermore, the output voltage of the sensor is relatively high compared to the noise level. Thus the output voltage of the sensor can be numerically differentiated to obtain $\dot{q}_j(t)$.

3. Control Design

In this section, following a study of actuator parameters and placement, a control law is developed for the 2-DOF flexible-link manipulator bonded with piezoelectric ceramics (Figure 4). Moreover a linear quadratic optimal controller, based on the dynamics of the flexible part, is used to obtain the input control signal for the PZT actuators. In addition to the control method, successful suppression of the dominant vibration modes depends on efficient use of the piezoelectric actuators. Therefore optimizing actuator parameters becomes an important issue.

3.1. Effect of system parameters and actuator placement

In this section, the effect of system parameters on the performance of a PZT actuator mounted on a flexible beam is studied. Since a PZT actuator has limited torque generation capability, it is desirable to maximize the performance of the actuator used for suppressing vibrations. Toward this end, let us consider the dynamic equation that is governed by the flexible modes (i.e., $\Phi_{qq}\ddot{q} + \Omega q = \tau_z$). For this model, re-written in state-space form, the controllability Grammian matrix is calculated. The principal directions of the controllability Grammian matrix, W_c, span a sub-space of reachable states at time t_1, from zero initial state at time t_0, by a bounded amount of input energy. More precisely, this can be stated as follows [7]:

Let S_x be the set of all reachable states at time t_1 from zero initial state at time t_0 by constrained inputs with unit energy $\|u(t)\| = 1$. The set S_x is the n dimensional ellipsoid:

$$S_x = \{x \mid x = U_c \Sigma_c u(t), \|u(t)\| \leq 1\}$$

where U_c and $\Sigma_c = diag(\sigma_n, \ldots, \sigma_2, \sigma_1)$ are obtained from the singular value decomposition of the $W_c(t_0, t_1) = U_c \Sigma_c U_c^T$. Also, the minimum amount of energy required to reach a state $\tilde{q} = (q, \dot{q})^T$ at time t_1 from zero initial condition at time t_0, is given by:

$$E \equiv \int_{t_0}^{t_1} u^T u dt = \tilde{q}^T W_c^{-1}(t_0, t_1) \tilde{q} = \sum_{i=1}^{n} \frac{(U_{c_i}^T \tilde{q})^2}{\sigma_i}$$

The above energy is a sum of the potential and the kinetic energies associated with each state. Each term in the above summation is proportional to the inverse of one singular value. In particular, the inverse singular values $\frac{1}{\sigma_1}$ and $\frac{1}{\sigma_n}$ denote the range of maximum and minimum control energies to attain a unit state at the terminal time from zero initial state. Therefore, minimizing the energy required for steering the system to an arbitrary state implies maximizing singular values $(\sigma_1, \ldots, \sigma_n)$ with respect to the parameter(s) under study such as the relative thickness of the PZT with respect to the beam, Young's modulus of elasticity, or the PZT location. Let us first look at the variations of the system singular values with respect to the thickness ratio of the beam and the actuator, i.e., t_h/t_z. Figure 1 shows such variations associated with the first vibration mode. Three different materials are considered. As an example, for steel the optimum thickness is found to be in the range $1.2 \leq t_h/t_z \leq 1.7$. The same optimum thickness ratio is obtained if these graphs are plotted for the other singular values associated with other vibration modes. An immediate implication of this fact is that a unique optimum thickness ratio can be found that maximizes all singular values simultaneously.

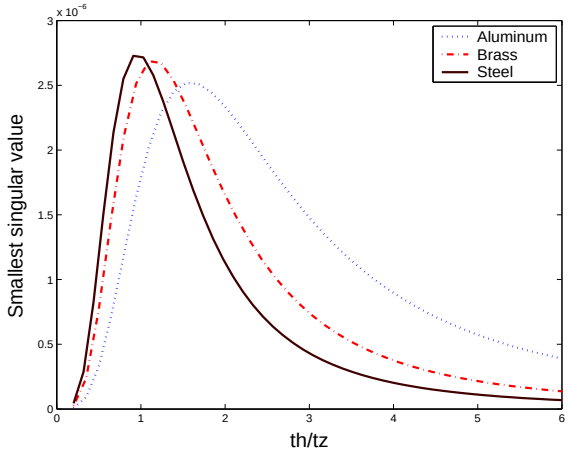

Figure 1. Variations of the singular values vs thickness ratio $\frac{t_h}{t_z}$

Next, the location of the actuator as one of the most important parameters, is studied. The total energy required to suppress an initial vibration in the system is a weighted sum of the inverse of the singular values. Each singular value corresponds to one mode of vibration considered in modeling. Thus, a minimum value of the control energy to steer a specific mode is obtained at the position where the associated singular value is maximum [6]. This corresponds to minimizing the energy required for suppressing that specific mode.

Along the same lines, the variation of the singular values associated with the first two modes of vibration with respect to the location of the actuator along the flexible beam is studied. The smaller singular value associated with the 1^{st} vibration mode (Figure 2(A)), has a maximum value close to the root of the beam. This is the optimum location of the actuator for the first vibration mode (i.e., $\frac{x_a}{L} \approx 0.1$). It is noteworthy that the optimum location for this mode is not exactly at the root of the beam. For the 2^{nd} mode, there are two local maxima (Figure 2(B)), one of which is at the root

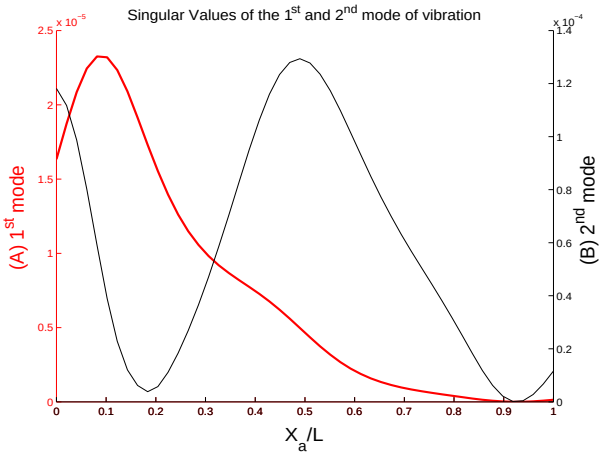

Figure 2. Variations of the singular values vs PZT location $\frac{x_a}{L}$

of the beam and the other one is at the mid-point. Also, increasing the length of the PZT improves its control authority on the 1^{st} vibration mode, while its optimum location mentioned above is unchanged. The effect of this parameter on the 2^{nd} mode is the same except for the fact that as the length is increased, the optimum location of the actuator moves toward the mid-point of the beam, where the corresponding singular value becomes maximum. More details can be found in [5]

3.2. Feedback Linearization

Here we briefly discuss the scheme used for controlling the system. The general idea is based on partial feedback linearization applied to flexible-link manipulators [8] [9]. A flexible link manipulator is not in general feedback linearizable, however, the system is locally input-output linearizable. In order to apply the input-output linearization technique to the flexible beam, let us consider the system dynamics as described in (4). This can be re-written as follows:

$$\begin{aligned}\ddot{\theta} &= h_{\theta\theta}\big(\tau_{motor} - v_\theta(r,\dot{r})\big) + h_{\theta q}\big(\tau_z - v_q(r,\dot{r}) - \Omega q\big)\\ \ddot{q} &= h_{\theta q}^T\big(\tau_{motor} - v_\theta(r,\dot{r})\big) + h_{qq}\big(\tau_z - v_q(r,\dot{r}) - \Omega q\big)\end{aligned} \tag{13}$$

where

$$H(r) = M^{-1}(r) = \begin{pmatrix} h_{\theta\theta} & h_{\theta q} \\ h_{\theta q}^T & h_{qq} \end{pmatrix} \tag{14}$$

Defining the output as:

$$y = \begin{pmatrix} \theta_1 \\ \theta_2 L + \delta(x,t)|_{x\approx L} \end{pmatrix} \tag{15}$$

and differentiating it with respect to time until the input vector appears, leads to the input-output description of the system in (13) as given below:

$$\ddot{y} = b(r,t)\tau_{motor} - a(r,\dot{r},t) \tag{16}$$

where

$$a(r,\dot{r},t) = b(r,t)v_\theta + (h_{\theta q} + \Phi_\varphi h_{qq})(v_q + \Omega q - \tau_z) \tag{17}$$
$$b(r,t) = h_{\theta\theta} + \Phi_\varphi h_{\theta q}^T$$

with

$$\Phi_\varphi = \begin{pmatrix} 0 \\ \varphi_1(L), \ldots, \varphi_n(L) \end{pmatrix}$$

Now suppose that there is a finite domain around the desired reference trajectory, y_d, in which $b(r,t)$ is nonsingular. This assumption is a controllability-like assumption for nonlinear systems and is guaranteed to hold when for instance $\Phi_\varphi = 0$. In that case, $b(r,t) = h_{\theta\theta}$ is positive-definite and therefore invertible. Thus in the neighborhood of $\Phi_\varphi = 0$, $b(r,t)$ is guaranteed to be invertible. Furthermore, let τ_{motor} take the following form:

$$\tau_{motor} = b^{-1}(r,t)(\tau_{new} + a(r,\dot{r},t)) \tag{18}$$

where τ_{new} is taken as a new input to the system. This results in the linearized input-output dynamics of the system as given by:

$$\ddot{y} = \tau_{new} \tag{19}$$

Also substituting τ_{motor} from (18) into the right-hand side of (13) yields

$$\ddot{q} = -p\Omega q + p\tau_z - pv_q + h_{\theta q}^T b^{-1}\tau_{new} \tag{20}$$

with:

$$p = h_{qq} - h_{\theta q}^T b^{-1}(h_{\theta q} + \Phi_\varphi h_{qq})$$

Let us now proceed as if (19) is the open-loop dynamics of a system to be controlled. Defining

$$\tau_{new} = \ddot{y}_d + K_p e + K_d \dot{e} \tag{21}$$

and substituting it into the right-hand side of (19) leads to the closed-loop error dynamics

$$\ddot{e} + K_d\dot{e} + K_p e = 0 \tag{22}$$

where

$$e = y_d - y \tag{23}$$

and K_p and K_d can be chosen to make the closed-loop system have the desired damping behavior. Moreover, the dynamics of the flexible part can be utilized to obtain a proper control law for the secondary input (i.e., the PZT actuators). It then follows from (9) and (20) that

$$\dot{\tilde{q}} = A_q\tilde{q} + B_q v(t) + d_q \tag{24}$$

where

$$A_q = \begin{pmatrix} 0 & I \\ -p\Omega & 0 \end{pmatrix} \qquad B_q = \begin{pmatrix} 0 \\ p\Delta \end{pmatrix}$$

$$d_q = \begin{pmatrix} 0 \\ -pv_q + h_{\theta q}^T b^{-1}\tau_{new} \end{pmatrix}$$

$$\tilde{q} = (q_1(t), \ldots, q_n(t), \dot{q}_1(t), \ldots, \dot{q}_n(t))^T$$

Then, a linear quadratic optimal controller can be used to obtain the feedback control signal $v(t) = K_q\tilde{q}$, to damp out the residual vibrations.

3.3. Friction Compensation

A friction model is especially important in applications involving high-precision motion control, where the friction force needs to be adequately compensated for in order to improve the transient performance and to reduce steady-state tracking errors. It also ensures smooth control signals and allows for using smaller feedback gains. A dynamic model of friction can be obtained using LuGre's model of friction. This model incorporates a single continuous state to model presliding displacement [3]. However, in our case, it was found that a steady-state model of the friction based on LuGre's model can yield consistent results.

For each motor of the 2-DOF manipulator a separate friction model was obtained to match the experimental data. Then the models were included in the control law as a feed-forward term. The friction force characteristic of the linear motor is different from that of the rotary motor. The linear motor has larger stiction friction F_{s_l} than Coulomb friction F_{c_l}. Also there is a considerable amount of viscous friction as the manipulator speeds up. The behavior of the linear motor is different during acceleration and deceleration. Therefore two different functions were used for positive and negative acceleration, i.e.,

$$\begin{aligned} &\text{if } \operatorname{sgn}(\dot{\theta}_1) \neq \operatorname{sgn}(\ddot{\theta}_1) \\ &F_{F_l} = \operatorname{sgn}(\dot{\theta}_1)(F_{c_l} + (F_{s_l} - F_{c_l})e^{-\alpha_l|\dot{\theta}_1|}) + \beta_l\dot{\theta}_1 \\ &\\ &\text{otherwise} \\ &F_{F_l} = F_m(\tfrac{2}{1+e^{-\lambda\dot{\theta}_1}} - 1) \end{aligned} \tag{25}$$

where F_{c_l} and F_{s_l} are the Coulomb and stiction levels, α_l determines the transition of friction force between F_{c_l} and F_{s_l} and β_l accounts for the viscous friction. F_m is chosen so that the the friction force is continuous. Figure 3A represents this model compared with the experimental data obtained from the linear motor.

The same procedure was followed in obtaining a friction model for the rotary motor. However experimental results revealed that in this case, friction characteristics could be captured only by including the velocity of the motor in the model, i.e.,

$$F_{F_r} = \operatorname{sgn}(\dot{\theta}_2)(F_{c_r} + (F_{s_r} - F_{c_r})e^{-\alpha_r|\dot{\theta}_2|}) + \beta_r\dot{\theta}_2 \tag{26}$$

All parameters in this model can be defined in the same way as for the linear motor. Comparison between this model and the experimental data obtained from the rotary motor are shown in Figure 3B.

Using the graphs in Figure 3, the parameters of the steady-state model can be appropriately selected. Table 1 lists these parameters for the linear and rotary motor respectively.

Having obtained the friction force, its value is added to the right-hand side of (18) as a feed-forward term.

4. Experimental Results

In order to examine the performance of the control algorithm, a flexible link bonded with a pair of PZT actuators, as shown in Figure 4, was built and mounted on top of a 2-DOF manipulator. A small PZT ceramic was also used as a sensor in order to obtain the modal information $(q_1, ..., q_n)$ of the flexible part.

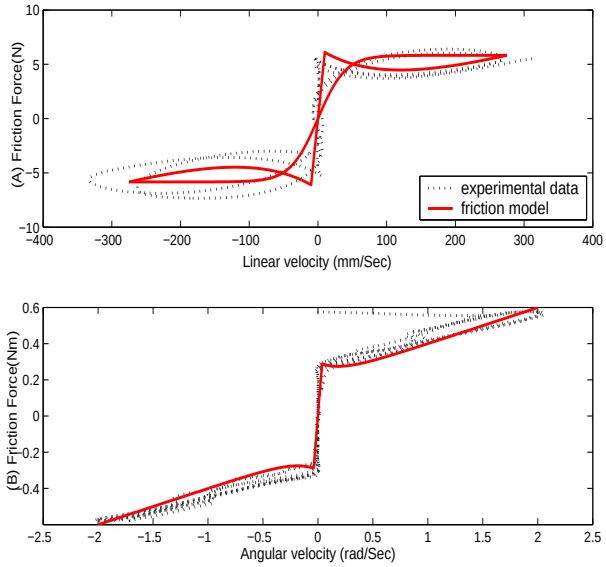

Figure 3. Steady-State friction force vs velocity

Table 1. Friction Force Parameters

	F_c	F_s	α	β	λ
Linear Motor	4.0	6.5	-0.1	0.05	0.1
Rotary Motor	0.15	0.4	-5.0	0.18	-

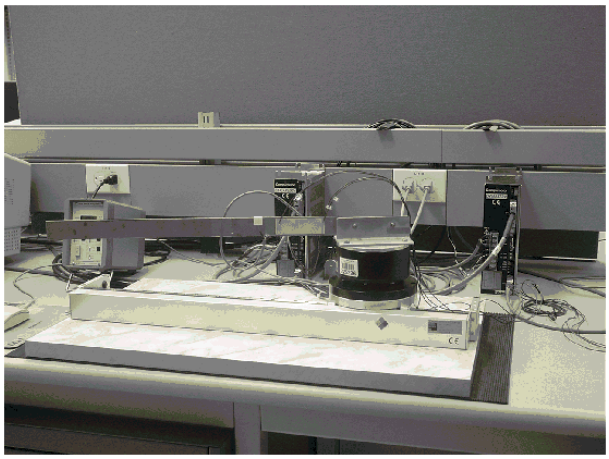

Figure 4. 2DOF flexible manipulator bonded with PZT's

The physical parameters of the flexible link and each actuator are listed in Table 2. The gain matrices K_p and K_d were set such that critical damping behavior of the tracking error was satisfied. Also K_q was obtained such that, in addition to suppressing

Table 2. System Parameters

	Link	**PZT Act.**
Material	Steel	
Modulus (N/m^2)	$E : 19.5 \times 10^{10}$	$E_z : 7.14 \times 10^{10}$
Length (m)	$L : 0.45$	$L_z : 0.0765$
Thickness (m)	$t_h : 0.001$	$t_z : 0.0005$
Width (m)	$w : 0.0285$	$w_z : 0.0285$
Density (Kg/m^3)	$\rho : 7800$	$\rho_z : 7650$
Charge Const. (m/volt)		$d_{31} : 250 \times 10^{-12}$
Actuators	**Linear**	**Rotary**
Max. Force/Torque	90 (N)	4 (Nm)
Max. Speed	2 (m/s)	2.5 (r/s)
Weight	1.4 (Kg)	3 (Kg)
Encoder Resolution	1×10^6 (p/m)	655360 (p/r)
Rotor Inertia		0.0025 (Kgm^2)

the residual vibrations at the end point of the link, the applied voltage to the PZT actuators remained within the maximum permissible voltage range.

A PC, running the Windows operating system, was used to implement the control strategy written in the C language. A sampling rate of 1 msec was used. A Multimedia timer (winmm.lib) that interrupted the program at the specified rate, was used under User mode of the Windows environment. The timer can trigger the control algorithm periodically (CALLBACK routine), yet it runs its own thread at the TIME_CRITICAL level which is the highest priority under User mode. In this way, the system can keep track of time while the control algorithm is being executed.

In order to show the effectiveness of the nonlinear control scheme, the performance of the system was tested experimentally. The desired trajectories to be tracked by the linear motor and the end point of the flexible link, were defined. The performance of the system using a linear PD controller with no PZT actuation and no friction compensation as shown in Figure 5 was used for comparison purposes. Figures 5(A,C,E) show the position of the linear motor, the angular position of the link and the deflection of the link respectively. Figures 5(B,D,F) show the corresponding torques applied to each motor and the PZT voltage.

As observed, the linear PD controller cannot successfully deal with flexibility in the system. However, the nonlinear controller, by including a model of the system in the control law, handles this problem efficiently. Figure 6 illustrates this fact. In this case, the manipulator is moved twice as fast as in the linear controller case, yet the performance of the system in terms of flexible link vibrations is still considerably

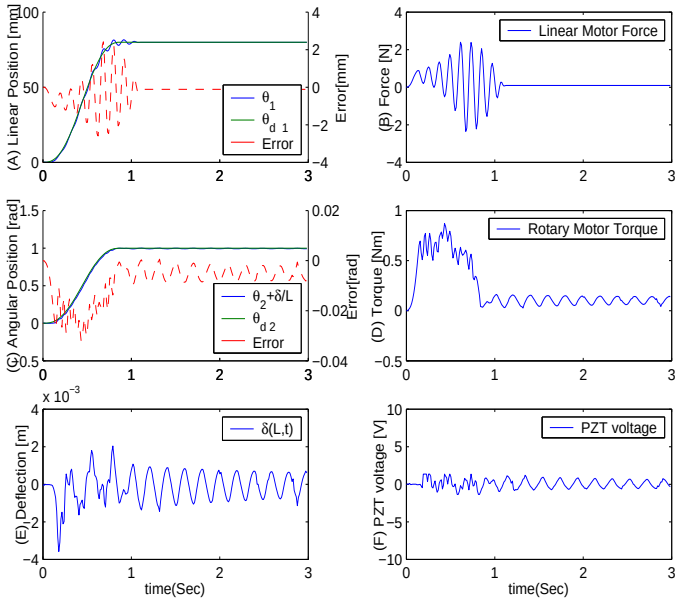

Figure 5. Performance of the linear PD controller

improved.

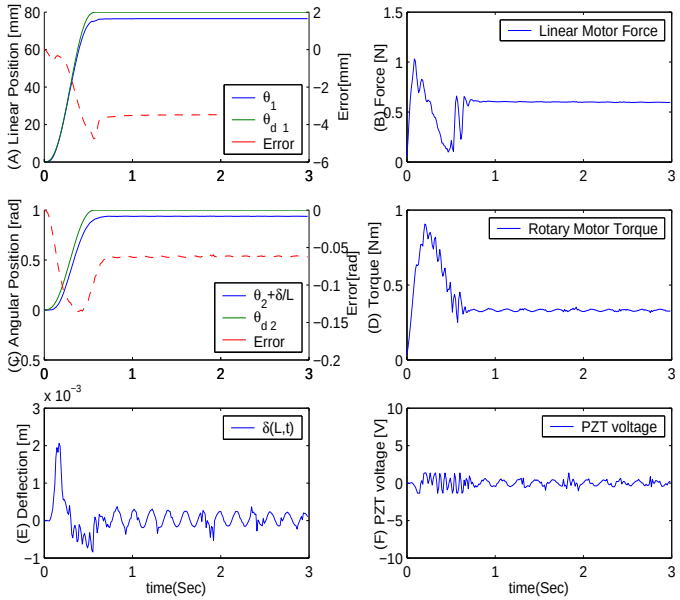

Figure 6. Performance of the nonlinear controller

In order to show the advantage of using PZT actuators, the performance of the nonlinear algorithm with PZT actuation is obtained as shown in Figure 7.

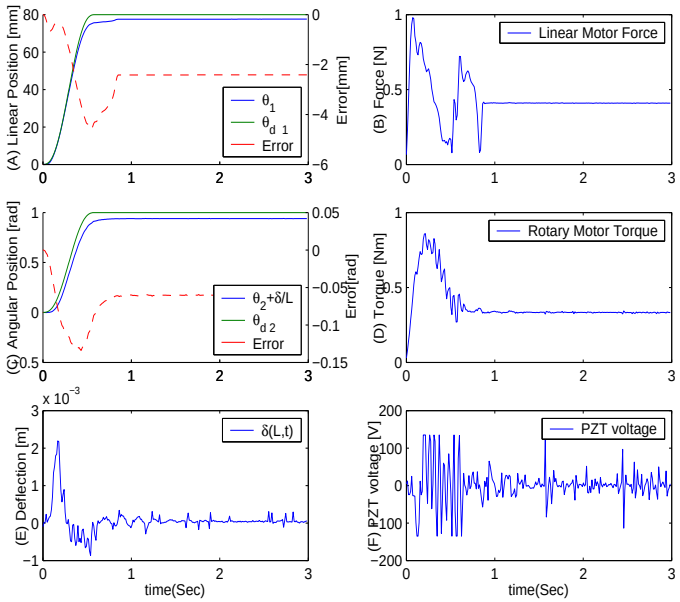

Figure 7. Performance of the nonlinear controller with PZT

Although residual vibrations at the end point of the link have been considerably attenuated, the performance of the system in terms of the tracking error may need further improvment. It is noteworthy that the PZT actuation most effectively, occurs when the motors decelerate at the end of the trajectory and the flexible link tends to vibrate. On the other hand, during tracking the desired trajectory the nonlinear algorithm is the most effective part in preventing vibrations in the system. Comparison of the maximum amplitude of vibration in the linear case (Figure 5E, maximum deflection = 4mm) and the nonlinear case (Figure 7E, maximum deflection = 2mm) explains this fact. To alleviate the tracking error problem, a friction compensation term is added to the control law. This term is calculated from the desired velocities in light of the fact that the tracking errors remain sufficiently small. As shown in Figure 8, including this term in the control law results in smaller tracking errors. By taking advantage of the PZT actuators, all performance requirements in terms of speed of manipulation and vibration of the link are satisfied.

5. Conclusions

In this paper, the utilization of piezoelectric actuators for suppressing vibrations in flexible-link manipulators was studied. A model for a 2-DOF flexible manipulator actuated with piezo-ceramics was derived. A non-linear control scheme based on partial feedback linearization was implemented, which incorporates a PZT actuator as a secondary input to the system. A steady-state model for the friction force was obtained and included in the control law. Experimental results were given to illustrate the effectiveness of the control algorithm in suppressing vibrations without sacrificing accuracy or speed.

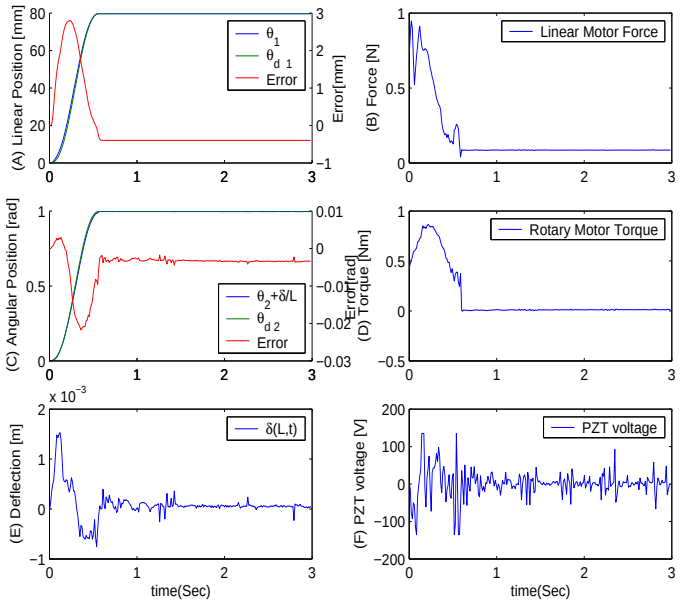

Figure 8. Performance of the nonlinear controller with PZT actuation and friction compensation

Acknowledgement

This work was partly performed at the Integrated Manufacturing Technologies Institute of the National Research Council of Canada in London, Ontario, Canada. The assistance provided by IMTI staff, in particular Mr. Dave Kingston and Dr. Mile Ostojic, is greatly appreciated.

References

[1] T. Bailey and J. E. Hubbard, "Distributed piezoelectric-polymer active vibration control of a cantilever beam," *Journal of Guidance, Control and Dynamics*, vol. 8, no. 5, pp. 605–611, 1986.

[2] E. F. Crawley and J. D. Luis, "Use of piezoelectric actuators as elements of intelligent structures," *American Institute of Aeronautics and Astronautics*, vol. 25, no. 10, pp. 1373–1385, 1987.

[3] C. C. de Wit, H. Olsson, K. J. A. ström, and P. Lischinsky, "A new model for control of systems with friction," *IEEE Transactions on Automatic Control*, vol. 43, no. 8, pp. 1189–1191, 1995.

[4] S. Hanagud, M. B. de Noyer, H. Luo, D. Henderson, and K. S. Nagaraja, "Tail buffet alleviation of high performance twin tail aircraft using piezo-stack actuators," *American Institute of Aeronautics and Astronautics*, vol. 40, no. 4, pp. 619–627, 2002.

[5] M. R. Kermani, M. Moallem, and R. Patel, "Parameter selection and control design for vibration suppression using piezoelectric transducers," *Control Engineering Practice, IFAC Journal*, accepted February 2003.

[6] M. R. Kermani, M. Moallem, and R. V. Patel, "Optimizing the performance of piezoelectric actuators for active vibration control," in *Proc. IEEE International Conference on Robotics and Automation*, vol. 3, Washington DC, 2002, pp. 2375–2380.

[7] K. B. Lim and W. Gawronski, *Control and Dynamic Systems, Advances in Theory and Applications*. New York: Academic Press, 1993, vol. 57, ch. Actuator and sensor placement for control of flexible structures, pp. 109–152.

[8] M. Moallem and R. Patel, "Optimal placement of smart actuators for vibration control of a flexible-link manipulator," in *American Control Conference*, Arlington, VA, 2001, pp. 941–946.

[9] M. Moallem, R. Patel, and K. Khorasani, *Flexible-Link Robot Manipulators: Control Techniques and Structural Design*. London: Springer-Verlag, 2000.

[10] B. Patnaik, G. R. Heppler, and D. Wang, "Stability analysis of a piezoelectric vibration controller for an euler-bernoulli beam," in *American Control Conference*, San Francisco, CA, 1992.

[11] J. Piedboeuf, "Six methods to model a flexible beam rotating in the vertical plane," in *Proc. IEEE International Conference on Robotics and Automation*, vol. 3, Seoul, Korea, 2001, pp. 2832–2839.

[12] J. B. Smits and W. Choi, "The constituent equations of piezoelectric heterogeneous bimorphs," *IEEE Transactions on Ultrasonics, Ferroelectrics and Frequency Control*, vol. 38, no. 3, pp. 256–270, 1991.

[13] A. V. Srinivasan and D. McFarland, *Smart Structure Analysis and Design*. UK: Cambridge University Press, 2001.

[14] D. Sun and J. K. Mills, "Study on piezoelectric actuators in control of a single-link flexible manipulator," in *Proc. IEEE International Conference on Robotics and Automation*, vol. 2, Detroit, MI, 1999, pp. 849–854.